Chiral or not chiral? A case study of the hexanuclear metalloprisms [Cp(6)M(6)(micro(3)-tpt-kappaN)(2)(micro-C2O4-kappaO)(3)]6+ (M = Rh, Ir, tpt = 2,4,6-tri(pyridin-4-yl)-1,3,5-triazine)

GOVINDASWAMY, Padavattan, *et al*.

Abstract

Cationic hexarhodium and hexairidium complexes with a trigonal prismatic architecture have been synthesised in good yield by self-assembly of the dinuclear oxalato-bridged complexes [Cp(2)M(2)(micro-C(2)O(4)-kappaO)Cl(2)] (M = Rh; 1: Ir; 2) with 2,4,6-tri(pyridine-4-yl)-1,3,5-triazine (tpt) in the presence of AgO(3)SCF(3). The trigonal prismatic cations [Cp(6)Rh(6)(micro(3)-tpt-kappaN)(2)(micro-C(2)O(4)-kappaO)(3)](6+) (3) and [Cp(6)Ir(6)(micro(3)-tpt-kappaN)(2)(micro-C(2)O(4)-kappaO)(3)](6+) (4) have been isolated as their triflate salts. The single-crystal X-ray structure analysis of [3][O(3)SCF(3)](6) shows two enantiomers in the racemic crystal (space group C2/c), the chirality being due to a twist of the two tpt units. By contrast, the single-crystal X-ray structure analysis of [4][O(3)SCF(3)](6) shows a perfectly eclipsed conformation of the tpt units, so that is not chiral in the crystal state (space group Fd3[combining macron]c). However, in solution, enantiodifferentiation in the presence of the chiral anion Delta-BINPHAT is observed by (1)H NMR spectrometry not only in the case of 3, but also in the case of 4. [...]

UNIVERSITÉ
DE GENÈVE

Chiral or not chiral? A case study of the hexanuclear metalloprisms [Cp*$_6$M$_6$(μ$_3$-tpt-κ*N*)$_2$(μ-C$_2$O$_4$-κ*O*)$_3$]$^{6+}$ (M = Rh, Ir, tpt = 2,4,6-tri(pyridin-4-yl)-1,3,5-triazine)†

Padavattan Govindaswamy,[a] David Linder,[b] Jérôme Lacour,[b] Georg Süss-Fink[a] and Bruno Therrien*[a]

Cationic hexarhodium and hexairidium complexes with a trigonal prismatic architecture have been synthesised in good yield by self-assembly of the dinuclear oxalato-bridged complexes [Cp*$_2$M$_2$(μ-C$_2$O$_4$-κ*O*)Cl$_2$] (M = Rh; **1**: Ir; **2**) with 2,4,6-tri(pyridine-4-yl)-1,3,5-triazine (tpt) in the presence of AgO$_3$SCF$_3$. The trigonal prismatic cations [Cp*$_6$Rh$_6$(μ$_3$-tpt-κ*N*)$_2$(μ-C$_2$O$_4$-κ*O*)$_3$]$^{6+}$ (**3**) and [Cp*$_6$Ir$_6$(μ$_3$-tpt-κ*N*)$_2$(μ-C$_2$O$_4$-κ*O*)$_3$]$^{6+}$ (**4**) have been isolated as their triflate salts. The single-crystal X-ray structure analysis of [**3**][O$_3$SCF$_3$]$_6$ shows two enantiomers in the racemic crystal (space group *C*2/*c*), the chirality being due to a twist of the two tpt units. By contrast, the single-crystal X-ray structure analysis of [**4**][O$_3$SCF$_3$]$_6$ shows a perfectly eclipsed conformation of the tpt units, so that **4** is not chiral in the crystal state (space group *Fd*$\bar{3}$*c*). However, in solution, enantiodifferentiation in the presence of the chiral anion Δ-BINPHAT is observed by ^{1}H NMR spectrometry not only in the case of **3**, but also in the case of **4**. This suggests that the iridium derivative **4**, which is not chiral in the solid state, adopts chiral conformations in solution.

Introduction

The first successful resolution of a chiral coordination compound was achieved by Werner in 1911.[1] The Co(III) complex, *cis*-[CoBr(en)$_2$(NH$_3$)]$^{2+}$ (en = ethylenediamine) was resolved into two enantiomers by crystallisation of the 3-bromocamphor-10-sulfonate salt. This first example confirmed Werner's hypothesis that tetrahedral structures do not exert a monopoly in chirality and that a stereogenic element must not necessarily be an "asymmetric" carbon atom.[2] This is especially true in supramolecular chemistry, where chirality can be induced also by a dissymmetric arrangement of achiral building blocks. Presumably the simplest chirality element in three-dimensional architectures is caused by the rotation of a trigonal plane with respect to a second trigonal plane, typically octahedral *vs.* trigonal prism geometry.[3] Consequently, in a triangular prism, if the two planar triangular subunits are perfectly eclipsed, the assembled molecule is achiral. However, a slight deviation from the eclipsed conformation generates a "double-rosette" type chirality with *P* (clockwise) or *M* (counter clockwise) configuration.[4] Recently, we have shown the cationic triangular metalloprisms [(η^6-arene)$_6$Ru$_6$(μ$_3$-tpt-κ*N*)$_2$(μ-C$_2$O$_4$-κ*O*)$_3$]$^{6+}$ (arene = *p*-^{i}PrC$_6$H$_4$Me, C$_6$Me$_6$) containing bridging oxalato ligands to possess such a helicity. Moreover, a concerted rotation of the aromatic rings of the tritopic tpt subunits was observed creating an additional three-bladed propeller chirality with Δ (clockwise) or Λ (counter clockwise) configuration.‡[5] These two stereogenic elements were observed in the solid-state and are shown to persist in solution as evidenced by ^{1}H NMR experiments in the presence of the anionic chiral NMR solvating agent Δ-BINPHAT.[6]
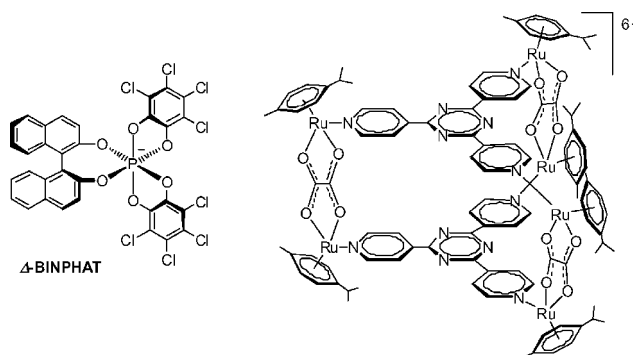

Thus, in the case of the cationic triangular metalloprism [(η^6-*p*-^{i}PrC$_6$H$_4$Me)$_6$Ru$_6$(μ$_3$-tpt-κ*N*)$_2$(μ-C$_2$O$_4$-κ*O*)$_3$]$^{6+}$, ^{1}H NMR analyses in the presence of Δ-BINPHAT anions revealed a clean enantiodifferentiation of the *p*-^{i}PrC$_6$H$_4$Me moieties but a broad resonance at room temperature for the pyridyl protons of the tpt subunits. These observations were rationalised by considering two decoupled stereodynamic phenomena: (i) a slow-on-the-NMR time scale "double rosette" interconversion (*P* ⇌ *M*) and (ii) a fast-on-the-NMR time scale propeller isomerism (Δ ⇌ Λ) (Scheme 1).[5] These observations raised the question of generality of such chiral conformations, and whether or not the stereodynamic phenomena observed for these hexaruthenium metalloprisms are unique.

[a]*Institut de Chimie, Université de Neuchâtel, Case postale 158, CH-2009, Neuchâtel, Switzerland. E-mail: bruno.therrien@unine.ch; Fax: +41 032 7182511; Tel: +41 0327182499*

[b]*Department of Organic Chemistry, University of Geneva, Quai E. Ansermet 30, CH-1211, Geneva 4, Switzerland*

‡ Both *M*/*P* and Δ/Λ descriptors are defined for the helical displacement viewed along the main *C*$_3$ axis.
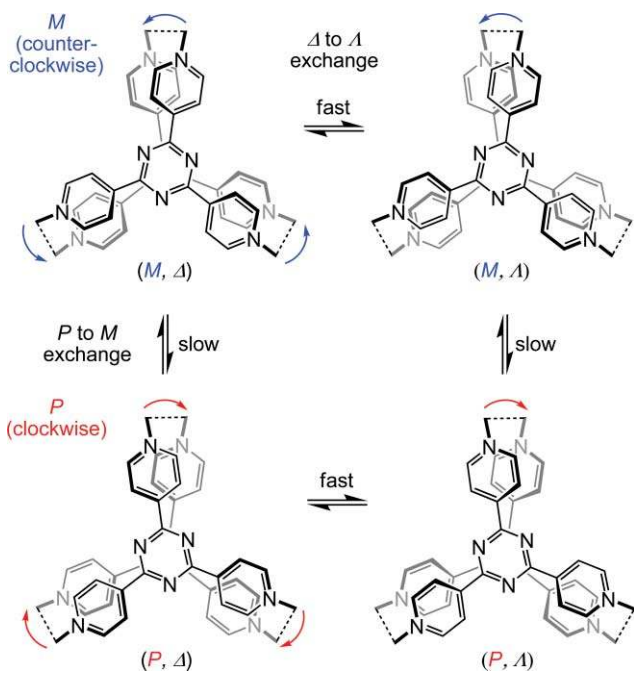
Scheme 1

In order to address this question, we synthesised triangular metalloprisms incorporating pentamethylcyclopentadienyl (Cp*) rhodium and iridium building blocks, bridged by oxalato ligands, and connected by two tpt subunits, isoelectronic to the hexaruthenium metalloprisms mentioned above. In this paper we report the synthesis, solid state structures and solution behaviour of $[Cp*_6Rh_6(\mu_3\text{-tpt-}\kappa N)_2(\mu\text{-}C_2O_4\text{-}\kappa O)_3][O_3SCF_3]_6$ and $[Cp*_6Ir_6(\mu_3\text{-tpt-}\kappa N)_2(\mu\text{-}C_2O_4\text{-}\kappa O)_3][O_3SCF_3]_6$.

Results and discussion

The hexametallic cations $[Cp*_6Rh_6(\mu_3\text{-tpt-}\kappa N)_2(\mu\text{-}C_2O_4\text{-}\kappa O)_3]^{6+}$ (**3**), and $[Cp*_6Ir_6(\mu_3\text{-tpt-}\kappa N)_2(\mu\text{-}C_2O_4\text{-}\kappa O)_3]^{6+}$ (**4**) are prepared following a two-step strategy, in which the new dinuclear oxalato complex $[Cp*_2Rh_2(\mu\text{-}C_2O_4\text{-}\kappa O)Cl_2]$ (**1**) as well as the known dinuclear oxalato complex $[Cp*_2Ir_2(\mu\text{-}C_2O_4\text{-}\kappa O)Cl_2]$ (**2**)[7] are used as metal "clips" (Scheme 2).
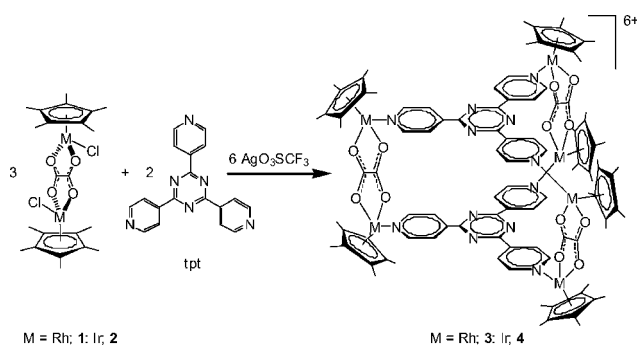
Scheme 2 Synthesis of metalloprisms **3** and **4**.

The dinuclear precursor complexes $[Cp*_2Rh_2(\mu\text{-}C_2O_4\text{-}\kappa O)Cl_2]$ (**1**) and $[Cp*_2Ir_2(\mu\text{-}C_2O_4\text{-}\kappa O)Cl_2]$ (**2**) were synthesised according to the previously published method of the analogous oxalato diruthenium complex $[(\eta^6\text{-}p\text{-}^iPrC_6H_4Me)_2Ru_2(\mu\text{-}C_2O_4\text{-}\kappa O)Cl_2]$[8]:

The dimetallic chloro complex $[Cp*M(\mu\text{-Cl})Cl]_2$ (M = Rh, Ir) reacts with $(NH_4)_2C_2O_4$ in a chloroform–methanol solution at 60 °C to give the corresponding complexes **1** and **2** in good yield. In the infrared spectra, only one very strong absorption at 1611 and 1622 cm^{-1} is observed, respectively, for the C=O stretching vibration of the oxalato bridging ligand. The molecular structure of **1** was determined by X-ray structural analysis. Crystals of **1** were obtained by the slow evaporation of a chloroform solution. An ORTEP drawing with the corresponding atom labelling scheme is shown in Fig. 1 together with selected bond lengths and angles.
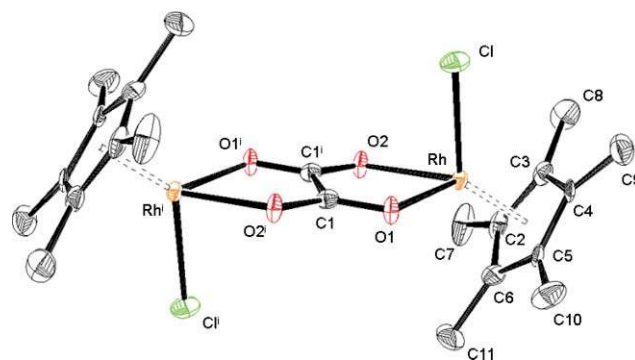

Fig. 1 ORTEP drawing of **1**, at 50% probability level, with hydrogen atoms being omitted for clarity. Selected bond lengths (Å) and angles (°): Rh–Rh^i 5.5628(7), Rh–Cl 2.3884(9), Rh–O(1) 2.149(2), Rh–O(2)^i 2.152(2); O(1)–Rh–O(2)^i 77.75(9), Cl–Rh–O(1) 88.12(7), Cl–Rh–O(2)^i 88.18(7). (i = 1 − x, −y, −z).

Complex **1** contains two rhodium metal centres bonded to a η^5-C_5Me_5 ligand, which are bridged by the dianionic $(C_2O_4)^{2-}$ ligand through its four oxygen atoms. The distance between the rhodium atom and the centre of the η^5-C_5Me_5 ring is 1.736 Å in **1**, whereas the corresponding Ir–C_5Me_5 distance is 1.731 Å in **2**.[7] The metal–metal separation of 5.5628(7) Å is comparable to those found in other oxalato bridged dinuclear M(arene) complexes (range 5.49–5.63 Å),[8,9] but slightly shorter to the corresponding M–M distance [5.585(1) Å] observed in the iridium complex $[Cp*_2Ir_2(\mu\text{-}C_2O_4\text{-}\kappa O)Cl_2]$ (**2**).[7] Despite the *trans* orientation of the two chloro ligands with respect to each other as shown by the X-ray structure analyses of **1** and **2**, it appears that, upon addition of AgO_3SCF_3, the unsaturated $Cp*_2M_2(\mu\text{-}C_2O_4\text{-}\kappa O)^{2+}$ intermediates are in a fast equilibrium between *cis* and *trans* geometries. The *cis* geometry is essential for the formation of the desired metalloprismatic arrangement.

The hexametallic complexes $[Cp*_6Rh_6(\mu_3\text{-tpt-}\kappa N)_2(\mu\text{-}C_2O_4\text{-}\kappa O)_3]^{6+}$ (**3**), and $[Cp*_6Ir_6(\mu_3\text{-tpt-}\kappa N)_2(\mu\text{-}C_2O_4\text{-}\kappa O)_3]^{6+}$ (**4**) are isolated and characterised as their triflate salts. The coordinatively unsaturated intermediates $Cp*_2M_2(\mu\text{-}C_2O_4\text{-}\kappa O)^{2+}$ formed upon addition of AgO_3SCF_3 presumably allow these moieties to adopt a *syn* geometry upon coordination to the tpt units. The two salts $[\mathbf{3}][O_3SCF_3]_6$ and $[\mathbf{4}][O_3SCF_3]_6$ turn out to be quite soluble and stable in $(CH_3)_2CO$ and MeOH, while they are only sparingly soluble in CH_2Cl_2 and $CHCl_3$. However, in CD_3CN, $[\mathbf{3}][O_3SCF_3]_6$ and $[\mathbf{4}][O_3SCF_3]_6$ show additional signals in their ^1H NMR spectrum attributed to species generated by coordination of CD_3CN ligands in line with cleavage of the tpt and oxalato bridges.

The ^1H NMR spectra of **3** and **4** display a similar signal pattern of the pyridyl protons, H_α and H_β. However, with respect

to the free tpt molecule, in **3** and **4**, the H_α signal is shifted to higher frequencies, whereas the H_β signal is shifted to lower frequencies (Fig. 2). The methyl protons of the Cp* groups appear as a singlet at 1.6–1.7 ppm, in **1–4**. The infrared spectra of **3** and **4** are dominated by absorptions of the coordinated 2,4,6-tri(pyridin-4-yl)-1,3,5-triazine ligand, which are only slightly shifted as compared to the free ligand [1515(s), 1374(s), 794(s), 641(s) cm^{-1}].[10] In addition to the tpt signals, strong absorptions attributed to the triflate anions [1260(s), 1030(s), 640(s) cm^{-1}][11] are observed in the infrared spectra of [**3**][O$_3$SCF$_3$]$_6$ and [**4**][O$_3$SCF$_3$]$_6$.
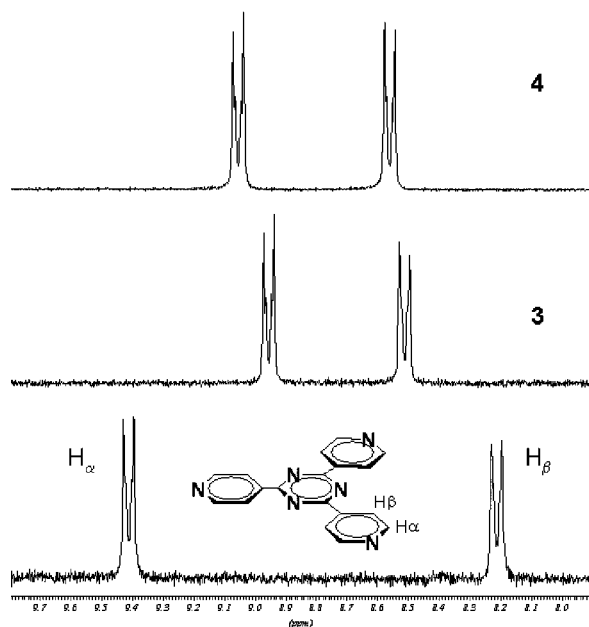

Fig. 2 ^{1}H NMR spectra (acetone-d$_6$) of tpt (bottom), **3** (middle) and **4** (top), showing the pyridyl region of the 2,4,6-tri(pyridin-4-yl)-1,3,5-triazine ligands.

The molecular structures of **3** and **4** were solved by X-ray structural analysis. Crystals of [**3**][O$_3$SCF$_3$]$_6$·(C$_6$H$_6$)$_6$ were obtained by the slow evaporation of an acetone–benzene solution, while crystals of [**4**][O$_3$SCF$_3$]$_6$, were obtained by the slow evaporation of an acetone solution. ORTEP drawings with the atom labelling scheme are shown in Fig. 3 and 4, respectively, together with selected bond lengths and angles.

The X-ray structure analyses of [**3**][O$_3$SCF$_3$]$_6$ and [**4**][O$_3$SCF$_3$]$_6$ show strong parallel π-stacking interactions between the aromatic rings of the tpt subunits (Fig. 5). The Rh–Rh (5.498(2) and 5.509(3) Å) and Ir–Ir (5.502(1) Å) distances are comparable to those found in the oxalato-bridged hexametallic metalloprisms [(η^6-p-^{i}PrC$_6$H$_4$Me)$_6$Ru$_6$(μ$_3$-tpt-κN)$_2$(μ-C$_2$O$_4$-κO)$_3$]$^{6+}$ (5.500(6) Å) and [(η^6-C$_6$Me$_6$)$_6$Ru$_6$(μ$_3$-tpt-κN)$_2$(μ-C$_2$O$_4$-κO)$_3$]$^{6+}$ (5.479(3) Å).[5] The centroid···centroid distances observed between corresponding aromatic rings of the π–π interacting systems (3.45 to 4.08 Å) are shorter than the theoretical value calculated for this stacking mode.[12] However, the triazine···triazine separations in **3** and **4** (3.45 and 3.46 Å) are comparable to the separation observed between the centroids of triazine rings of two independent tpt units in the crystal packing of [Cp*$_3$Ir$_3$(μ$_3$-tpt-κN){η^2-S$_2$C$_2$(B$_{10}$H$_{10}$)-κS}$_3$] (3.46 Å),[13] or between the triazine rings in the analogous tri-
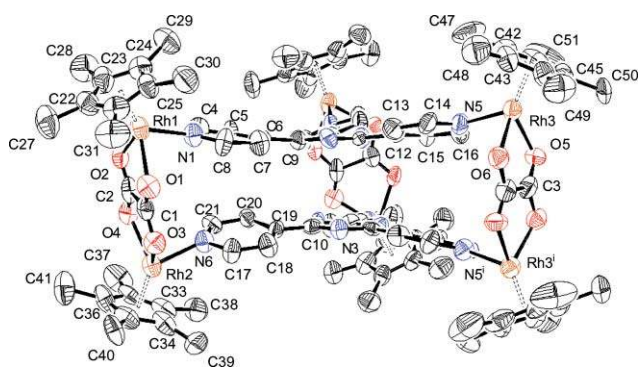

Fig. 3 ORTEP drawing of cation **3**, at 50% probability level, with hydrogen atoms, benzene molecules and O$_3$SCF$_3$ anions omitted for clarity. Selected bond lengths (Å) and angles (°): Rh(1)–Rh(2) 5.498(2), Rh(3)–Rh(3)^i 5.509(3), Rh(1)–N(1) 2.124(14), Rh(2)–N(6) 2.114(14), Rh(3)–N(5) 2.110(13), Rh(1)–O(1) 2.127(12), Rh(1)–O(2) 2.143(12), Rh(2)–O(3) 2.147(11), Rh(2)–O(4) 2.129(12), Rh(3)–O(5) 2.139(12), Rh(3)–O(6) 2.136(12); O(1)–Rh(1)–O(2) 77.9(5), O(3)–Rh(2)–O(4) 77.9(5), O(5)–Rh(3)–O(6) 78.8(5), N(1)–Rh(1)–O(1) 83.4(5), N(1)–Rh(1)–O(2) 84.5(5), N(6)–Rh(2)–O(3) 84.9(5), N(6)–Rh(2)–O(4) 88.3(5), N(5)–Rh(3)–O(5) 83.1(5), N(5)–Rh(3)–O(6) 86.9(5). (i = 1− x, y, 0.5 − z).
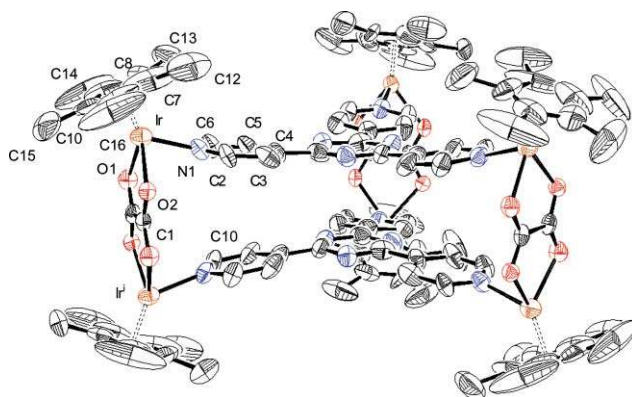

Fig. 4 ORTEP drawing of cation **4**, at 50% probability level, with hydrogen atoms and O$_3$SCF$_3$ anions omitted for clarity. Selected bond lengths (Å) and angles (°): Ir–Ir^i 5.502(1), Ir–N(1) 2.088(9), Ir–O(1) 2.144(7), Ir–O(2) 2.114(6), C(1)–O(1) 1.246(11), C(1)–O(2)^i 1.274(12), C(1)–C(1)^i 1.53(2); O(1)–Ir–O(2) 78.4(2), N(1)–Ir–O(1) 84.0(3), N(1)–Ir–O(2) 82.7(3). (i = z − 0.75, 2 − y, 0.75 + x).

angular metalloprism [(η^{6}C$_6$Me$_6$)$_6$Ru$_6$(μ$_3$-tpt-κN)$_2$(μ-C$_2$O$_4$-κO)$_3$]$^{6+}$ (3.42 Å).[5]

In the crystal packing of [**4**][O$_3$SCF$_3$]$_6$, no π-stacking interacting systems are observed between independent molecules. The empty spaces left between the cationic hexametallic cations are filled with disordered O$_3$SCF$_3$ anions and solvent molecules. However, in [**3**][O$_3$SCF$_3$]$_6$, crystallisation in an acetone–benzene mixture gives rise to a different packing in which benzene molecules are found around the metalloprism. One benzene molecule is located above the triazine subunits with a centroid···centroid separation of 3.52 Å, while a second benzene molecule is found to interact with a pentamethylcyclopentadienyl moiety with a centroid···centroid separation of 3.53 Å.

Interestingly, despite an almost identical centroid···centroid separation between the two triazine moieties in **3** and **4**, the two prismatic structures are quite different. In **4**, the tpt ligands adopt a
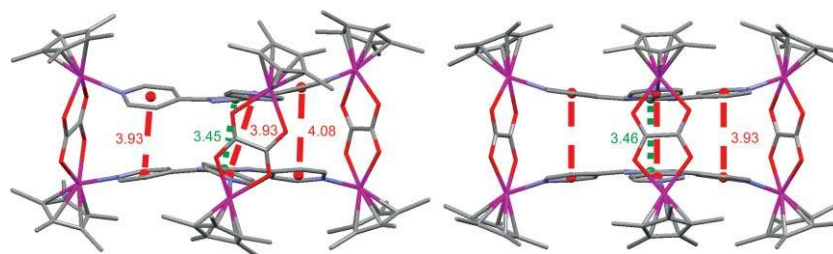
Fig. 5 Parallel π-stacking interactions (Å) between the aromatic rings of the tpt units in **3** (left) and **4** (right), pyridyl···pyridyl (red ---) and triazine···triazine (green ---).
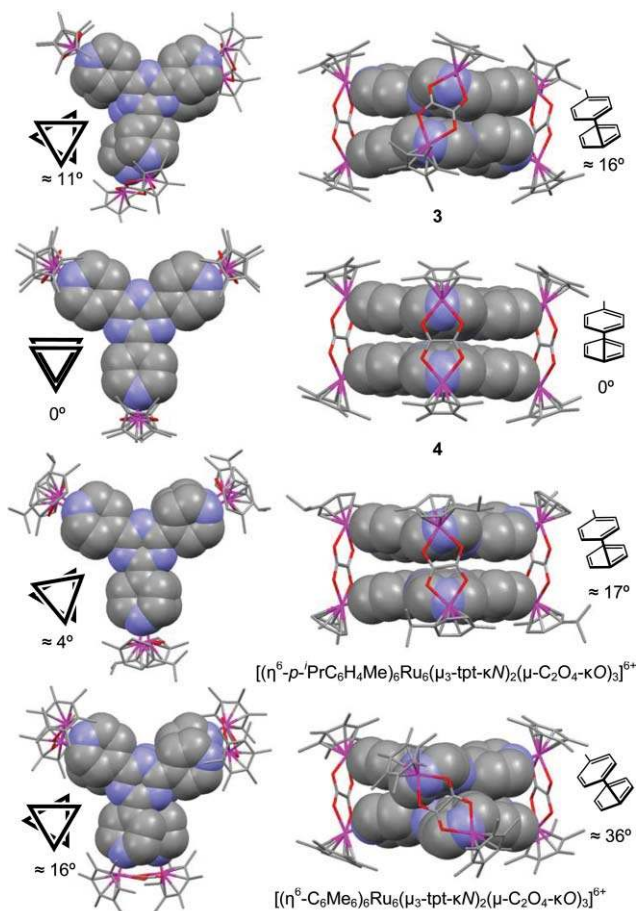
perfect eclipsed conformation, while in **3** a twist of the tpt subunits and a tilt of the pyridyl moieties are observed. Indeed, the twist angle between the two tpt subunits is about 11.0°, whereas the pyridyl rings of the two tpt units are tilted by 9.6, 11.7 and 20.8° out of the plane of the triazine ring.

This structural difference is fundamental with respect to chirality of the two hexacations. In [**4**][O_3SCF_3]$_6$, the two tpt units are perfectly eclipsed, so that cation **4** presents a threefold symmetry axis as well as a mirror plane perpendicular to it (Fig. 5 and 6).[14] By contrast, cation **3** shows, as the isoelectronic hexaruthenium metalloprisms,[5] a distinct distortion, the dimetallic oxalato "clips"
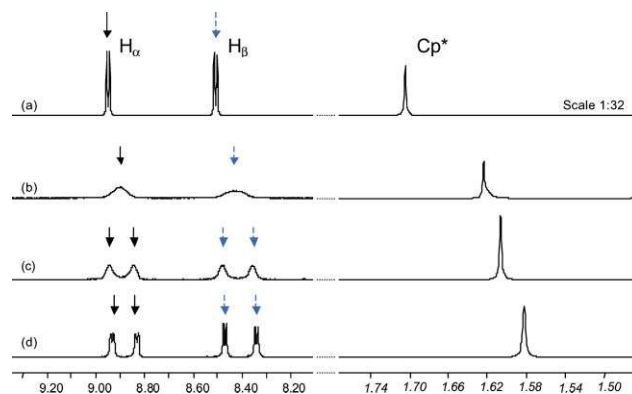
being twisted out of the plane of the tpt subunits, which gives rise to a "double-rosette" type helicity (Fig. 6). Furthermore, in **3** as in the isoelectronic hexaruthenium metalloprisms,[5] the pyridyl rings are tilted out of the plane of the triazine subunits, while in **4** they are not inclined at all. Thus, the hexairidium metalloprism **4** is not chiral in the solid state, in contrast to its rhodium homologue **3** (Fig. 6).

The ^{1}H NMR spectra of [**3**][O_3SCF_3]$_6$ and of [**4**][O_3SCF_3]$_6$ in acetone-d_6 show no signals indicating the presence of diastereotopic atoms or groups, neither at room temperature nor at low temperature (down to 223 K). Previously, the hexacoordinated phosphorus anion, bis(tetrachlorobenzenediolato)-mono([1,1′]-binaphthalenyl-2,2′-diolato)-phosphate(v) (BINPHAT), has been shown to be a general NMR chiral solvating, resolving and asymmetry-inducing reagent for organic and metallo-organic compounds.[6,15] Since it was particularly efficient for the enantiodifferentiation of the hexaruthenium metalloprisms,[5] we also preformed a NMR analysis of the salts [**3**][O_3SCF_3]$_6$ and [**4**][O_3SCF_3]$_6$ in the presence of [Bu$_4$N][Δ-BINPHAT].

Addition of [Bu$_4$N][Δ-BINPHAT] (3.0 equiv.) to an acetone-d_6 solution of [**3**][O_3SCF_3]$_6$ at 298 K (Fig. 7, spectrum b) leads to a significant broadening of the signals of the pyridyl protons (H$_\alpha$ and H$_\beta$) of the tpt subunits, while the signal for the methyl groups of the Cp* moieties remains sharp and unsplit at this temperature.§ Considering that the broad resonances at 298 K are the result

Fig. 6 Structural comparison (top view and side view) of [Cp*$_6$Rh$_6$(μ$_3$-tpt-κN)$_2$(μ-C$_2$O$_4$-κO)$_3$]$^{6+}$ (**3**), [Cp*$_6$Ir$_6$(μ$_3$-tpt-κN)$_2$(μ-C$_2$O$_4$-κO)$_3$]$^{6+}$ (**4**), [(η^6-p-^{i}PrC$_6$H$_4$Me)$_6$Ru$_6$(μ$_3$-tpt-κN)$_2$(μ-C$_2$O$_4$-κO)$_3$]$^{6+}$ and [(η^6-C$_6$Me$_6$)$_6$-Ru$_6$(μ$_3$-tpt-κN)$_2$(μ-C$_2$O$_4$-κO)$_3$]$^{6+}$.[5]

Fig. 7 ^{1}H NMR spectra (parts, 500 MHz, acetone-d_6) of [**3**][O_3SCF_3]$_6$: (a) 298 K, (b) 298 K, (c) 273 K, (d) 248 K; spectra (b), (c), (d) being measured in the presence of 3.0 equiv. of [Bu$_4$N][Δ-BINPHAT].

§ Addition of a larger amount of salt [Bu$_4$N][Δ-BINPHAT] leads to the precipitation of complex **3**. The precipitation is unselective as the two enantiomers of **3** remain in solution in a 1 : 1 ratio.

of stereodynamics, a variable-temperature NMR experiment for [**3**][O$_3$SCF$_3$]$_6$ was performed (248–298 K, acetone-d$_6$), see Fig. 7.

Upon cooling the solution to 248 K, the pyridyl signals become sharp and well resolved (Fig. 7, spectrum (d), giving rise to a split of the tpt signals ($\Delta\delta$ 0.10 and 0.14 ppm for H$_\alpha$ and H$_\beta$, respectively). This clearly confirms the presence of diastereomeric ion pairs in stereodynamic equilibrium and that the chirality observed in the solid state is maintained in solution. The kinetics of the racemisation are in the range of the NMR time scale at 298 K.[16] The signal for the methyl protons of the Cp* groups is shifted to lower frequencies as the temperature decreases ($\Delta\delta$ 0.10 ppm and 0.12 ppm at 298 K and 248 K, respectively).

Interestingly, addition of [Bu$_4$N][Δ-BINPHAT] to an acetone-d$_6$ solution of [**4**][O$_3$SCF$_3$]$_6$ at 298 K, also caused a splitting of the signals of the pyridyl protons ($\Delta\delta$ 0.17 and 0.21 ppm for H$_\alpha$ and H$_\beta$, respectively for 9.0 equiv. of Δ-BINPHAT, Fig. 8, spectrum (e)). As for **3**, the signal of the methyl protons of the Cp* groups is shifted but shows no split. These observations imply that two diastereomeric ion pairs are formed in solution with the enantiopure Δ-BINPHAT anion. Thus, in sharp contrast to its achiral solid state structure, complex **4** must adopt chiral conformations in solution.
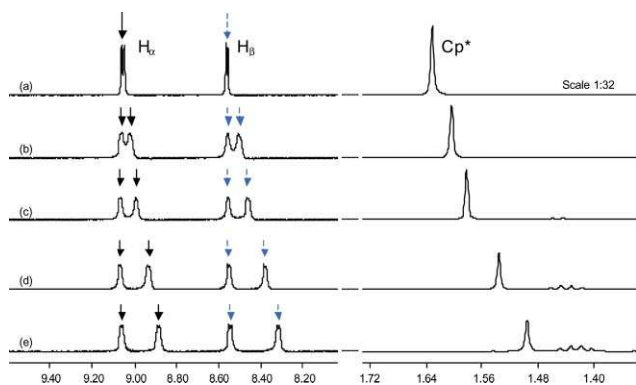
Fig. 8 ^{1}H NMR spectra (parts, 500 MHz, acetone-d$_6$) of [**4**][O$_3$SCF$_3$]$_6$ with (a) 0, (b) 1.0, (c) 2.0, (d) 5.0 and (e) 9.0 equiv. of [Bu$_4$N][Δ-BINPHAT].

To gain further insight into the behaviour in solution of cation **4** in the presence of Δ-BINPHAT anions, a titration was performed, see Fig. 8. It appears that, upon incremental addition of [Bu$_4$N][Δ-BINPHAT] (1.0 to 9.0 equiv.), only one enantiomeric conformation of **4** is strongly perturbed by the presence of the Δ-BINPHAT anion, the other showing a much reduced influence of the anion ($\Delta\delta_{max}$ −0.02 vs. −0.24 ppm for H$_\beta$ in the presence of 9.0 equiv. of the NMR reagent, Fig. 8, spectrum (f)). This result, indicating a dissymmetry in the ion pairing association of the conformers of **4** with Δ-BINPHAT anion, suggests that chiral recognition may be at play, although the lack of stereoselective induction upon salt formation disfavours this hypothesis.

These NMR experiments indicate that both complexes **3** and **4** adopt chiral conformations in solution at room temperature as well as at lower temperature. Based on the solid state molecular structure of **3** and the observations made previously for the ruthenium analogues,[5] it is more than probable that these conformations are either of the type "double rosette" ($P \rightleftharpoons M$) and/or propeller isomerism of the tpt subunits ($\Delta \rightleftharpoons \Lambda$). However, as the X-ray structure analysis of [**4**][O$_3$SCF$_3$]$_6$ revealed a complete lack of these

stereogenic elements in the solid state of **4**, it is, at this stage, not possible to ascertain the origin of the chirality of **4** observed in solution.

Conclusion

In conclusion, we have opened a simple and straightforward access to oxalato-bridged cyclopentadienyl rhodium and iridium metalloprisms. These metalloprisms show strong parallel π-stacking interactions between the tpt units as demonstrated by ^{1}H NMR spectroscopy and X-ray structure analysis. Moreover, the oxalato metalloprisms **3** and **4** give, in sharp contrast to the solid-state molecular structure of [**4**][O$_3$SCF$_3$]$_6$, rise to a chiral conformation in solution, as shown by the NMR spectrometric measurements in the presence of Δ-BINPHAT.

Experimental

General remarks

[Cp*Rh(μ-Cl)Cl]$_2$,[17] [Cp*Ir(μ-Cl)Cl]$_2$,[17] 2,4,6-tri(pyridin-4-yl)-1,3,5-triazine[18] and [Bu$_4$N][Δ-BINPHAT][6] are prepared according to published methods. All other reagents are commercially available and used as received. The ^{1}H and ^{13}C{^{1}H} NMR spectra are recorded on a Bruker AMX 400 spectrometer using the residual protonated solvent as internal standard. Infrared spectra are recorded on a Perkin-Elmer FTIR 1720X spectrometer. Microanalyses are performed by the Laboratory of Pharmaceutical Chemistry, University of Geneva (Switzerland).

Synthesis of complexes 1 to 4

[Cp*$_2$Rh$_2$(μ-C$_2$O$_4$-κO)Cl$_2$] (1). To a chloroform–methanol (1 : 1, 30 mL) solution of [Cp*Rh(μ-Cl)Cl]$_2$ (154.5 mg, 0.25 mmol) was added (NH$_4$)$_2$C$_2$O$_4$·H$_2$O (35.5 mg, 0.25 mmol). The mixture was refluxed for 6 h. After removal of the solvent under vacuum, the residue was dissolved in dichloromethane (15 mL). The resulting slurry was filtered to remove ammonium chloride salts. The solution was evaporated to dryness to give complex **1** as an orange solid. Yield 140 mg, (88%). ^{1}H NMR (400 MHz, CDCl$_3$): δ (ppm) = 1.70 (s, 30H, C$_5$Me$_5$); ^{13}C{^{1}H} NMR (100 MHz, CDCl$_3$): δ (ppm) = 172.26, 92.91, 9.38; IR (KBr, cm^{-1}): 1611(s) (CO). Anal. calcd for C$_{22}$H$_{30}$Cl$_2$O$_4$Rh$_2$: C, 41.60; H, 4.76. Found: C, 41.36; H, 4.87%.

[Cp*$_2$Ir$_2$(μ-C$_2$O$_4$-κO)Cl$_2$] (2). Prepared by the same procedure as described above for **1**, using [Cp*Ir(μ-Cl)Cl]$_2$ (199 mg 0.25 mmol) and (NH$_4$)$_2$C$_2$O$_4$·H$_2$O (35.5 mg 0.25 mmol). Yield 165 mg, (81%). ^{1}H NMR (400 MHz, CDCl$_3$): δ (ppm) = 1.67 (s, 30H, C$_5$Me$_5$); ^{13}C{^{1}H} NMR (100 MHz, CDCl$_3$): δ (ppm) = 174.53, 84.11, 9.63; IR (KBr, cm^{-1}): 1622(s) (CO). Anal. calcd for C$_{22}$H$_{30}$Cl$_2$O$_4$Ir$_2$: C, 32.47; H, 3.71. Found: C, 32.53; H, 3.82%.

[Cp*$_6$Rh$_6$(μ_3-tpt-κN)$_2$(μ-C$_2$O$_4$-κO)$_3$][O$_3$SCF$_3$]$_6$ ([3][O$_3$SCF$_3$]$_6$). A mixture of [Cp*$_2$Rh$_2$(μ-C$_2$O$_4$-κO)Cl$_2$] (**1**) (70 mg, 0.11 mmol) and AgO$_3$SCF$_3$ (59 mg, 0.23 mmol) in MeOH (20 mL) was stirred at room temperature for 2 h. The yellow solution was filtered to remove AgCl and after addition of 2,4,6-tri(pyridin-4-yl)-1,3,5-triazine (tpt) (23 mg, 0.073 mmol) the mixture was stirred at room temperature for 36 h. The solvent was removed under vacuum and the residue was taken up in dichloromethane (20 mL) and filtered.

Table 1 Crystallographic and selected experimental data for **1**, [**3**][O$_3$SCF$_3$]$_6$·(C$_6$H$_6$)$_6$ and [**4**][O$_3$SCF$_3$]$_6$

	1	[**3**][O$_3$SCF$_3$]$_6$·(C$_6$H$_6$)$_6$	[**4**][O$_3$SCF$_3$]$_6$
Chemical formula	C$_{22}$H$_{30}$Cl$_2$O$_4$Rh$_2$	C$_{144}$H$_{150}$F$_{18}$N$_{12}$O$_{30}$Rh$_6$S$_6$	C$_{108}$H$_{114}$F$_{18}$Ir$_6$N$_{12}$O$_{30}$S$_6$
Formula weight	635.18	3680.58	3747.67
Crystal system	Monoclinic	Monoclinic	Cubic
Space group	$P2_1/c$	$C2/c$	$Fd\bar{3}c$
Crystal color and shape	Orange block	Yellow block	Yellow cube
Crystal size/mm	0.18 × 0.16 × 0.15	0.15 × 0.14 × 0.12	0.15 × 0.15 × 0.15
a/Å	8.2751(6)	25.082(2)	50.159(6)
b/Å	8.8048(7)	20.029(2)	
c/Å	16.703(1)	33.218(2)	
β/°	93.804(9)	110.095(6)	
V/Å^3	1214.3(2)	15672(2)	126196(26)
Z	2	4	32
T/K	173(2)	173(2)	173(2)
D_c/g cm^{-3}	1.737	1.560	1.578
μ/mm^{-1}	1.604	0.792	5.204
Scan range/°	2.4 < θ < 25.95	1.33 < θ < 25.19	1.99 < θ < 25.17
Unique reflections	2333	13863	4537
Reflections used [$I > 2\sigma(I)$]	2048	4220	2074
R_{int}	0.0389	0.1676	0.0709
Final R indices [$I > 2\sigma(I)$]^a	0.0228, wR_2 0.0552	0.1092, wR_2 0.2626	0.0536, wR_2 0.1284
R indices (all data)	0.0303, wR_2 0.0789	0.2556, wR_2 0.3246	0.1076, wR_2 0.1435
Goodness-of-fit	1.270	0.854	0.812
Max, Min Δρ/e Å^{-3}	0.930, −1.151	1.856, −1.206	0.583, −0.715

^{a} Structures were refined on F_o^2: $wR_2 = [\sum[w(F_o^2 - F_c^2)^2]/\sum w(F_o^2)^2]^{1/2}$, where $w^{-1} = [\sum(F_o^2) + (aP)^2 + bP]$ and $P = [\max(F_o^2, 0) + 2F_c^2]/3$.

The filtrate was dried under vacuum to give an orange-yellow solid. Yield 85 mg, (72%). ^{1}H NMR (400 MHz, acetone-d$_6$): δ (ppm) = 8.94 (dd, 12H, $^3J_{H-H}$ = 6.56 Hz, $^4J_{H-H}$ = 1.48 Hz, H$_\alpha$), 8.49 (dd, 12H, H$_\beta$), 1.69 (s, 90H, C$_5$Me$_5$); ^{13}C{^{1}H} NMR (100 MHz, acetone-d$_6$): δ (ppm) = 171.23, 170.59, 153.07, 144.54, 126.66, 96.29, 8.27; IR (KBr, cm^{-1}): 1622(s) (CO), 1520(s), 1383(s), 1260(s), 1158(s), 1031(s), 810(s), 638(s). Anal. calcd for C$_{108}$H$_{114}$N$_{12}$O$_{30}$S$_6$F$_{18}$Rh$_6$: C, 40.39; H, 3.58; N, 5.23. Found: C, 40.49; H, 3.24; N, 5.06%.

[Cp*$_6$Ir$_6$(μ_3-tpt-κN)$_2$(μ-C$_2$O$_4$-κO)$_3$][O$_3$SCF$_3$]$_6$ ([4][O$_3$SCF$_3$]$_6$). Prepared by the same procedure as described above for **3**, using [Cp*$_2$Ir$_2$(μ-C$_2$O$_4$-κO)Cl$_2$] (**2**) (90 mg 0.11 mmol), AgO$_3$SCF$_3$ (59 mg, 0.23 mmol) and tpt (23 mg, 0.074 mmol). Yield 95 mg, (68%). ^{1}H NMR (400 MHz, acetone-d$_6$): δ (ppm) = 9.03 (dd, 12H, $^3J_{H-H}$ = 5.20 Hz, $^4J_{H-H}$ = 1.52 Hz, H$_\alpha$), 8.54 (dd, 12H, H$_\beta$), 1.62 (s, 90H, C$_5$Me$_5$); ^{13}C{^{1}H} NMR (100 MHz, acetone-d$_6$): δ (ppm) = 174.82, 170.30, 153.51, 144.82, 127.31, 87.78, 8.33; IR (KBr, cm^{-1}): 1631(s) (CO), 1520(s), 1384(s), 1259(s), 1163(s), 1032(s), 812(s), 640(s). Anal. calcd for C$_{108}$H$_{114}$N$_{12}$O$_{30}$S$_6$F$_{18}$Ir$_6$: C, 34.61; H, 3.07; N, 4.48. Found: C, 35.16; H, 3.25; N, 4.14%.

Titration experiments with [Bu$_4$N][Δ-BINPHAT]

^{1}H NMR data were obtained on a Bruker AMX-500 spectrometer. Chemical shifts δ are given in ppm and reported relative to Me$_4$Si and residual solvent peak. To a standard NMR tube were added 1.8 mg of [**3**][O$_3$SCF$_3$]$_6$ (0.5 µmol) along with 0.75 mL of acetone-d$_6$ (6.7 × 10^{-4} mmol L^{-1}). A solution of [Bu$_4$N][Δ-BINPHAT] (52 mg, 5.10^{-2} mmol) in 0.75 mL of acetone-d$_6$ (6.7 × 10^{-2} mol L^{-1}) was prepared in a vial fitted with a rubber septum. 10 µL portions of this solution (6.7 × 10^{-4} mmol, 1.0 equiv.) were sequentially added to the NMR tube which was shaken for 5 min before recording the ^{1}H NMR spectra at 293 K.

X-Ray crystallographic study

Crystals of [Cp*$_2$Rh$_2$(μ-C$_2$O$_4$-κO)Cl$_2$] (**1**), [Cp*$_6$Rh$_6$(μ_3-tpt-κN)$_2$(μ-C$_2$O$_4$-κO)$_3$][O$_3$SCF$_3$]$_6$ ([**3**][O$_3$SCF$_3$]$_6$·(C$_6$H$_6$)$_6$) and [Cp*$_6$Ir$_6$(μ_3-tpt-κN)$_2$(μ-C$_2$O$_4$-κO)$_3$][O$_3$SCF$_3$]$_6$ ([**4**][O$_3$SCF$_3$]$_6$) were mounted on a Stoe Mark II-Image Plate Diffraction System, using Mo-Kα graphite monochromated radiation, image plate distance 135 mm, 2θ range from 1.7–51.6°, D_{max}–D_{min} = 23.99–0.82 Å. The structures were solved by direct methods using the program SHELXS-97.[19] Refinement and all further calculations were carried out using SHELXL-97.[19] In all cases, the H atoms were included in calculated positions and treated as riding atoms using the SHELXL default parameters. Examination of the structure of [**4**][O$_3$SCF$_3$]$_6$ with PLATON[20] reveals voids between the anions and cations. Indeed, in [**4**][O$_3$SCF$_3$]$_6$ voids corresponding to solvent molecules and disordered triflate molecules were found. Therefore, a new data set corresponding to omission of the missing solvent and anions was generated with the SQUEEZE algorithm[21] and the structure was refined to convergence. In all cases, the non-H atoms were refined anisotropically, using weighted full-matrix least-squares on F^2. Crystallographic details are summarised in Table 1. Fig. 1, 3 and 4 were drawn with ORTEP[22] while Fig. 5 and 6 used MERCURY.[23]

CCDC reference numbers: 650992 [Cp*$_2$Rh$_2$(μ-C$_2$O$_4$-κO)Cl$_2$] (**1**), 650993 [Cp*$_6$Rh$_6$(μ_3-tpt-κN)$_2$(μ-C$_2$O$_4$-κO)$_3$][O$_3$SCF$_3$]$_6$ ([**3**][O$_3$SCF$_3$]$_6$ · (C$_6$H$_6$)$_6$) and 650994 [Cp*$_6$Ir$_6$(μ_3-tpt-κN)$_2$(μ-C$_2$O$_4$-κO)$_3$][OSO$_2$CF$_3$]$_6$ ([**4**][O$_3$SCF$_3$]$_6$).

Notes and references

1 A. Werner, *Ber. Dtsch. Chem. Ges.*, 1911, **44**, 1887.
2 G. B. Kauffman, *Coord. Chem. Rev.*, 1974, **12**, 105.
3 S. Alvarez, M. Pinsky and D. Avnir, *Eur. J. Inorg. Chem.*, 2001, 1499.
4 (*a*) A. Ikeda, H. Udzu, Z. Zhong, S. Shinkai, S. Sakamoto and K. Yamaguchi, *J. Am. Chem. Soc.*, 2001, **123**, 3872; (*b*) L. J. Prins, R. Hulst, P. Timmerman and D. N. Reinhoudt, *Chem.–Eur. J.*, 2002, **8**, 2288; (*c*) R. W. Saalfrank, B. Demleitner, H. Glaser, H. Maid, D. Bathelt, F. Hampel, W. Bauer and M. Teichert, *Chem.–Eur. J.*, 2002, **8**, 2679; (*d*) H. Fenniri, B.-L. Deng and A. E. Ribbe, *J. Am. Chem. Soc.*, 2002, **124**, 11064; (*e*) S. Hiraoka, K. Harano, T. Tanaka, M. Shiro and M. Shionoya, *Angew. Chem., Int. Ed.*, 2003, **42**, 5182; (*f*) M. G. J. ten Cate, M. Omerović, G. V. Oshovsky, M. Crego-Calama and D. N. Reinhoudt, *Org. Biomol. Chem.*, 2005, **3**, 3727.
5 P. Govindaswamy, D. Linder, J. Lacour, G. Süss-Fink and B. Therrien, *Chem. Commun.*, 2006, 4691.
6 J. Lacour, A. Londez, C. Goujon-Ginglinger, V. Buss and G. Bernardinelli, *Org. Lett.*, 2000, **2**, 4185.
7 D. B. Grotjahn, H. C. Lo, J. Dinoso, C. D. Adkins, C. Li, S. P. Nolan and J. L. Hubbard, *Inorg. Chem.*, 2000, **39**, 2493.
8 H. Yan, G. Süss-Fink, A. Neels and H. Stoeckli-Evans, *J. Chem. Soc., Dalton Trans.*, 1997, 4345.
9 (*a*) F. Bottomley, I. J. B. Lin and P. S. White, *J. Organomet. Chem.*, 1981, **212**, 341; (*b*) S. H. Dale and M. R. J. Elsegood, *Acta Crystallogr., Sect. C*, 2006, **62**, m166.
10 H.-G. Biedermann and K. Z. Wichmann, *Z. Naturforsch., B: Anorg. Chem., Org. Chem.*, 1974, **29**, 360.
11 D. H. Johnston and D. F. Shriver, *Inorg. Chem.*, 1993, **32**, 1045.
12 S. Tsuzuki, K. Honda, T. Uchimura, M. Mikami and K. Tanabe, *J. Am. Chem. Soc.*, 2002, **124**, 104.
13 J.-Q. Wang, C.-X. Ren and G.-X. Jin, *Chem. Commun.*, 2005, 4738.
14 This is analogous to what has been observed in the solid state for hex-ametallic chloro-bridged metalloprisms, $[(\eta^6\text{-}p\text{-}^i\text{PrC}_6\text{H}_4\text{Me})_6\text{Ru}_6(\mu_3\text{-tpt-}\kappa N)_2(\mu\text{-Cl})_6]^{6+}$ and $[(\eta^6\text{-C}_6\text{Me}_6)_6\text{Ru}_6(\mu_3\text{-tpt-}\kappa N)_2(\mu\text{-Cl})_6]^{6+}$. See: P. Govindaswamy, G. Süss-Fink and B. Therrien, *Organometallics*, 2007, **26**, 915.
15 (*a*) J. Lacour and V. Hebbe-Viton, *Chem. Soc. Rev.*, 2003, **32**, 373; (*b*) J. Lacour and R. Frantz, *Org. Biomol. Chem.*, 2005, **3**, 15.
16 An approximate energy barrier of 14.7 kcal mol^{-1} ($\pm 5\%$) for the enantiomerisation of **3** can be calculated considering the classical formula $\Delta G^{\ddagger} = RT_c (22.96 + \ln (T_c/\Delta v)$ with $T_c = 298\text{K}$ and $\Delta v = 50$ Hz; Δv being the difference in frequency between the speared signals of protons H_{β} and T_c the coalescence temperature.
17 C. White, A. J. Oliver and P. M. Maitlis, *J. Chem. Soc., Dalton Trans.*, 1973, 1901.
18 H. L. Anderson, S. Anderson and J. K. M. Sanders, *J. Chem. Soc., Perkin Trans. 1*, 1995, 2231.
19 G. M. Sheldrick, *SHELX suite of programs for crystal structure solution and refinement*, University of Göttingen, Germany, 1997.
20 A. L. Spek, *J. Appl. Crystallogr.*, 2003, **36**, 7.
21 A. L. Spek and P. von der Sluis, *Acta Crystallogr., Sect. A*, 1990, **46**, 194.
22 L. J. Farrugia, *J. Appl. Crystallogr.*, 1997, **30**, 565.
23 I. J. Bruno, J. C. Cole, P. R. Edgington, M. Kessler, C. F. Macrae, P. McCabe, J. Pearson and R. Taylor, *Acta Crystallogr., Sect. B*, 2002, **58**, 389.